ACS Sustainable Chemistry & Engineering

Research Article

pubs.acs.org/journal/ascecg

Processing, Structure, and Properties of Lignin- and CNT-Incorporated Polyacrylonitrile-Based Carbon Fibers

H. Clive Liu,[†,‡] An-Ting Chien,[†] Bradley A. Newcomb,[†] Yaodong Liu,[†] and Satish Kumar*[,†,‡]

[†]School of Materials Science and Engineering, Georgia Institute of Technology, 801 Ferst Drive NW, MRDC-1, Atlanta, Georgia 30332, United States

[‡]Renewable Bioproducts Institute, Georgia Institute of Technology, 500 10th Street NW, Atlanta, Georgia 30332, United States

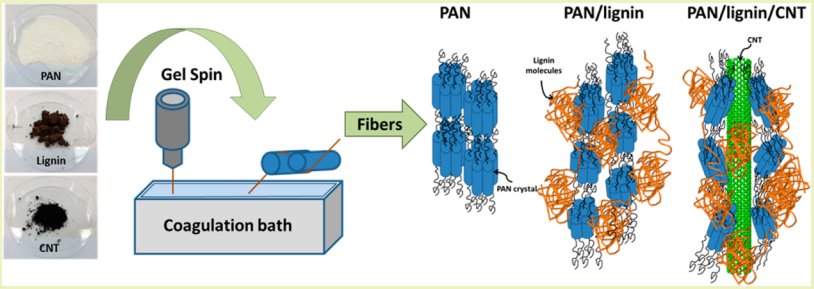

ABSTRACT: Composite fibers comprised of lignin, polyacrylonitrile (PAN), and carbon nanotubes (CNT) were successfully fabricated by gel-spinning technology. Wide angle X-ray diffraction (WAXD), infrared spectroscopy, and thermal characterizations were used to identify the effects of lignin and CNT on the physical structure and stabilization process of gel-spun precursor fibers. PAN, PAN/lignin, and PAN/lignin/CNT precursors have been converted to carbon fibers under identical stabilization and carbonization conditions. When carbonized at 1100 °C, PAN/lignin carbon fiber exhibits comparable mechanical properties to PAN carbon fiber. Raman spectroscopy studies suggested differences between the carbon fibers when lignin and CNTs were incorporated.

KEYWORDS: *Polyacrylonitrile PAN, Lignin, Fiber, Carbon fiber, Carbon nanotubes, CNT*

INTRODUCTION

Carbon fibers have excellent mechanical properties and relatively low density and are therefore employed as reinforcing materials in aerospace structures, windmill blades, sport equipment, and automotive applications. With its versatility, the carbon fiber demand has been growing steadily.[1,2] Today, polyacrylonitrile PAN-based fibers are the most dominant precursor of carbon fiber, and the cost of PAN fibers contributes 30% to 50% to the carbon fiber cost.[3] Biomacromolecules have been considered as alternative precursor fiber candidates. Early carbon fibers (in the 1960s) were produced from cellulosic fibers such as rayon. However, due to relatively low properties, rayon-based carbon fibers are no longer commercially manufactured. As the byproduct of the pulp and paper industry and also the second most abundant biomacromolecule on earth, lignin has been proposed as a cost-effective alternative for a carbon fiber precursor as a renewable feedstock.[4,5] However, mechanical properties of the lignin-based carbon fibers to date are relatively low, as compared to the PAN-based carbon fibers.[6−9] Lignin fibers are typically processed by melt spinning, while PAN fibers are processed from solution.[5,7] To integrate the advantages of the good mechanical performance of PAN and the cost advantage of lignin, PAN/lignin blend fibers have been spun.[10,11] However, it has been reported that incorporating lignin into polymer composites could result in lower mechanical properties. Melt-extruded polyethylene and polypropylene with lignin (up to 30 wt %) exhibited lower tensile strength with increasing lignin content.[12] Melt-spun PLA/lignin fibers also showed decreasing tensile strength and modulus values when lignin content was increased up to 90 wt %.[13] Industrial feasibility of solution-spun PAN/lignin carbon fiber production was investigated by Zoltek in partnership with Weyerhaeuser under a DOE-funded program.[14,15] PAN/lignin precursor fibers with different lignin content (up to 45%), PAN molecular weights, and solution solid contents were reported.[14] Although carbon fibers up to 25 wt % lignin were in successful production to meet targeted properties, mechanical performance of composite carbon fibers were still lower than those reported for the control PAN carbon fibers due to increasing microvoids in composite fibers with increasing lignin content.[14,16] Possible causes of voids were attributed to low solution viscosities, type of lignin employed, and phase separation during coagulation.[5] Pores in PAN/lignin fiber were also observed in a more recent study as well.[17] Additionally, batch thermal oxidation studies suggested significant differences in the stabilization process between PAN and PAN/lignin composite fibers.[14,17] However, under-

Received: February 19, 2015
Revised: July 21, 2015
Published: August 19, 2015

DOI: 10.1021/acssuschemeng.5b00562
ACS Sustainable Chem. Eng. 2015, 3, 1943−1954

standing of the lignin interaction with polymers and its conversion process to carbon is still limited.[18]

Carbon nanotubes (CNTs) have been known for influencing mechanical properties, thermal shrinkage, polymer orientation, and crystal size, as well as thermal and electrical conductivity of both gel-spun PAN precursors and carbon fibers.[19−24] In 2011, Baker et al. reported melt-spun lignin/CNT fibers.[25] Although no mechanical properties were originally provided, in a later study, enhancements in tensile strength and tensile modulus for both precursors and carbon fibers were reported with the addition CNTs.[5] However, absolute mechanical property values were not reported. More recently, Teng et al. reported electrospun softwood kraft lignin/CNT/poly(ethylene oxide) (PEO) and lignin/PEO composite fibers and their carbonized products.[26] Solids including 1−6 wt % of CNT were prepared in dimethylformamide, and PEO (1 wt %) was added to improve spinnability. Tensile strength and modulus of the lignin/CNT/PEO precursor were lower than those for the corresponding values for lignin/PEO products when CNT loading was more than 4 wt %, and tensile strength and moduli of carbonized lignin/CNT/PEO were lower than those of lignin/PEO carbon fiber mats in all cases. Lower mechanical properties of carbon fiber mats with the addition of CNT were reported and attributed to poor interfacial interaction as shown from debonding between CNT and the surrounding matrix according to TEM images of thermally stabilized and carbonized products.[26] Teng et al. further reported that lignin from different treatments or fractionations could critically affect intermolecular interactions with CNTs in solution.[27] However, the interactions between lignin and CNT during fiber spinning and in the final fiber remain unclear and are of interest in the current study.

In this work, the authors present both PAN/lignin and PAN/lignin/CNT precursor systems and their carbon fibers utilizing gel-spinning technique. This study is an attempt to understand the PAN/lignin and PAN/lignin/CNT precursors and to investigate the effects of lignin on polymer fiber structure and thermal stabilization and carbonization behavior in order to fully understand PAN/lignin and PAN/lignin/CNT systems for industrial practice. Processing parameters, structure and thermal characterization, and mechanical performance are reported, and the effects of lignin and CNT on the fiber structure and precursor as well as carbon fiber fabrication process are discussed.

EXPERIMENTAL SECTION

Materials. Sulfur free, annual plant lignin powder (Protobind 2400) from the soda pulping process was provided by GreenValue (Media, PA) and was selected for composite fiber processing based on previously reported favorable properties of the PAN/lignin blend films.[11,28] Homopolymer polyacrylonitrile (250 000 g/mol) was acquired from Exlan Co. (Japan), and multiwalled carbon nanotubes with an average diameter of 21.0 ± 3.1 nm were purchased from CheapTubes.com (Brattleboro, VT).[22] DMAc was obtained from Sigma-Aldrich Co. and used as received. As-received lignin powder (ash content ∼1%) was washed with diluted HCl and distilled water repeatedly until the ash content was lower than 0.3%. Washed lignin was then dried under vacuum at 60 °C overnight before use.

Solution Preparation. Three types of solutions (PAN, PAN/lignin, and PAN/lignin/CNT) were prepared for spinning. For the PAN solution, 14 g of PAN was dissolved in 100 mL DMAc at 80 °C. For the PAN/lignin solution, 14 g of PAN and 6 g of lignin were mixed and then dissolved in DMAc at the same conditions. To prepare for the PAN/lignin/CNT composite solutions, a total of three CNT batches were added separately into the PAN/lignin solution. Each CNT batch was prepared in DMAc at a concentration of 250 mg/300 mL under 24 h of sonication (Cole-Parmer 8891R-DTH, 80 W, 43 kHz). PAN (17.5 g) and lignin (7.5 g) solids were dissolved in 100 mL of DMAc at 80 °C before the CNT batches (total solid of 0.75 g) were added. The weight ratio for PAN/lignin and PAN/lignin/CNT were 70:30 and 70:30:3, respectively. Excessive DMAc solvent from the CNT batches were evaporated by vacuum distillation. All prepared solutions were maintained at 60 °C before spinning.

Fiber Spinning. Fibers were gel-spun through a spinnerette with a 200 μm diameter hole on a spinning system built by Hills, Inc. PAN and PAN/lignin/CNT fibers were spun at the spinning temperature of 85 °C, while PAN/lignin fiber was spun at 60 °C for better spinnability, as this fiber exhibited poor spinnability at 85 °C. The solid contents of PAN, PAN/lignin (70/30 weight ratio), and PAN/lignin/CNT (70/30/3 weight ratio) for successful fiber spinning were 14, 20, and 25.75 g/dL, respectively. Fiber spinning for PAN/lignin (70/30 weight ratio) was also attempted at a lower solid content of 14 g/dL, and for PAN/lignin/CNT (70/30/3 weight ratio), it was attempted at 14 and 20 g/dL concentrations and was not successful. Note that for the PAN/lignin blend, the solid content for fiber spinning was notably higher than that for the homopolymer PAN, but the solution temperature at which the PAN/lignin blend fiber could be spun was lower than that for the PAN or the PAN/lignin/CNT blend. This was the first indication of the interactions between PAN/lignin and PAN/lignin/CNT. As shown in the Results and Discussion section, spectroscopic (FTIR and Raman) as well as physio-mechanical (DSC, TMA, DMA) methods provide further evidence of interaction in these binary and ternary blends.

All fibers were spun into methanol coagulation bath maintained at −50 °C with an air gap of 3 cm. As-spun fibers were stored in a methanol bath at −30 °C for over 12 h and subsequently drawn at room temperature followed by drawing in a glycerol bath at 165 °C. While the max draw ratio of PAN fiber could reach over 20, the max draw ratio of PAN/lignin fiber was 13. With the incorporation of CNT, the max draw ratio of PAN/lignin/CNT fiber was improved to 20. In this study, for a meaningful comparison between the three types of fibers, a draw ratio of 13 was selected for all fibers. Dynamic mechanical analysis was performed on the precursor fiber at 0.1, 1, and 10 Hz frequencies using RSA III solids analyzer. Thirty-filament bundles were used for the test at a 25.4 mm gauge length with a heating rate of 1 °C/min from 30 to 200 °C. Thermal shrinkage was studied via a thermo-mechanical analyzer (TMA Q400, TA Instruments) at a stress of 10 MPa with a heating rate of 0.5 °C/min to 280 °C. Tensile properties were tested via FAVIMAT on single filaments at a 25.4 mm gauge length. The strain rates for tensile testing for precursors and carbon fibers were 1%/s and 0.1%/s, respectively. For each trial, more than 15 samples were tested. Differential scanning calorimetry was conducted on the precursor fibers (TA Instrument Q200) in an oxidative environment of an air flow of 50 mL/min and at a heating rate of 5 °C/min. To study the fiber structure, WAXD patterns were obtained by a Rigaku Micromax-002 and Rigaku IV++ detecting system with operating parameters of 45 kV, 0.65 mA, and λ = 1.5418 Å. Diffraction patterns were analyzed using AreaMax V1.00 and MDI Jade 6.1. For each sample, peak analysis was performed more than once to exclude experimental errors. FTIR spectra of the precursor and stabilized fibers were collected on Spectrum One from PerkinElmer with a resolution of 4 cm^{-1}. A tube furnace (Lindberg, 51668-HR, Blue M Electric) was used for fiber stabilization and carbonization. Raman spectra of carbon fibers were obtained using a 785 nm laser on a Raman microscope system from HORIBA Scientific. For Raman spectroscopy, carbon fibers were mounted onto paper tabs and fixed with cyanoacrylate adhesive at both ends. Raman spectra were taken with an objective of magnitude 100× at 5.6 mW laser power with an exposure time of 12 s in the VV mode, and the fiber samples were aligned parallel to the polarizer and analyzer. PeakFit software was used to analyze the acquired Raman spectra with Gaussian−Lorentzian curve fitting. SEM images were collected using a Zeiss Ultra 60 FE-SEM at an accelerating voltage of 2 kV.

DOI: 10.1021/acssuschemeng.5b00562
ACS Sustainable Chem. Eng. 2015, 3, 1943−1954

RESULTS AND DISCUSSION

Effects of Lignin on Polymer Packing and Orientation. The WAXD patterns of the as-spun fiber with a draw ratio (DR) of 2 and a precursor with total DR of 13 are shown in Figures 1 and 2, respectively. The structural parameters of as-spun and drawn precursor fibers are given in Table 1. Lignin is completely amorphous, and PAN has both amorphous and crystalline peaks in the X-ray diffraction. Compared to the PAN fiber, PAN/lignin fiber shows smaller crystal size and lower crystallinity. Studies have shown that the packing of PAN polymer chains changes from orthorhombic to hexagonal under drawing, which results in a ratio of *d*-spacing of $2\theta \approx 17°$ to *d*-spacing of $2\theta \approx 30°$ ($d_{17°}/d_{30°}$) approaching to $3^{1/2}$ (1.732).[29−32] At a draw ratio of 2, *d*-spacing of $2\theta \approx 17°$ and *d*-spacing of $2\theta \approx 30°$ of PAN fibers are 5.28 and 3.19 Å, respectively ($d_{17°}/d_{30°}$ = 1.656). With the incorporation of lignin, PAN/lignin fiber shows *d*-spacings of 5.26 Å at $2\theta \approx 17°$ and 3.22 Å at $2\theta \approx 30°$. This yields $d_{17°}/d_{30°}$ = 1.635, which deviates from the PAN hexagonal packing ratio of 1.732. While the fibers are further drawn to a draw ratio of 13, PAN fiber shows *d*-spacings at $2\theta \approx 17°$ and $2\theta \approx 30°$ to be 5.25 and 3.03 Å, respectively and leads to $d_{17°}/d_{30°}$ of 1.733. On the other hand, PAN/lignin fiber (draw ratio 13) shows smaller *d*-spacings of 5.22 and 3.02 Å, with $d_{17°}/d_{30°}$ of 1.726, which is slightly lower than the expected value of 1.732 for hexagonal packing. This suggests that the presence of lignin molecules in the fiber influences the PAN packing.

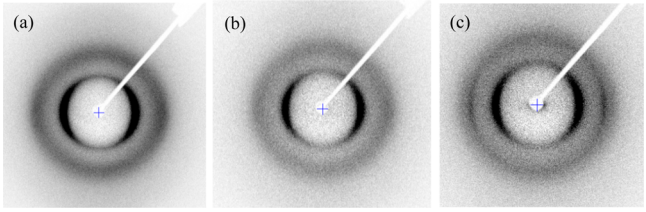

Figure 1. WAXD patterns of the as spun precursors (DR = 2) of (a) PAN, (b) PAN/lignin, and (c) PAN/lignin/CNT fibers.

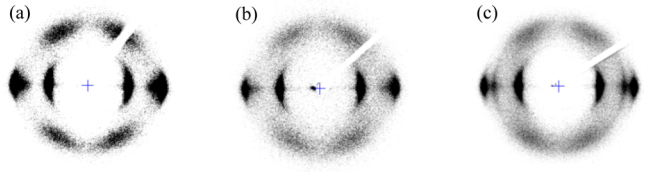

Figure 2. WAXD patterns of precursor fibers (DR = 13) of (a) PAN, (b) PAN/lignin, and (c) PAN/lignin/CNT fibers.

Table 1. Structural Parameters of PAN and PAN/Lignin/CNT Precursors

draw ratio = 2	PAN	PAN/lignin	PAN/lignin/CNT
crystallinity[a] (%)	53	49	52
L$2\theta \approx 17°$[b] (nm)	3.6	3.0	3.1
f_{PAN}[c]	0.57	0.55	0.54
d-spacing ($2\theta \approx 17°$) (Å)	5.28	5.26	5.23
d-spacing ($2\theta \approx 30°$) (Å)	3.19	3.22	3.19
$2\theta_{meridional\ scan}$ (deg)	39.65	39.86	39.43
$d_{17°}/d_{30°}$	1.656	1.635	1.640
draw ratio = 13	**PAN**	**PAN/lignin**	**PAN/lignin/CNT**
crystallinity[a] (%)	65	60	57
L$2\theta \approx 17°$[b] (nm)	10.5	8.3	9.5
f_{PAN}[c]	0.88	0.86	0.85
d-spacing ($2\theta \approx 17°$) (Å)	5.25	5.22	5.23
d-spacing ($2\theta \approx 30°$) (Å)	3.03	3.02	3.02
$2\theta_{meridional\ scan}$ (deg)	39.25	39.35	39.13
$d_{17°}/d_{30°}$	1.733	1.726	1.728

[a]Crystallinity is only with respect to the PAN crystal since lignin molecules are completely amorphous.[81] [b]Crystal size of PAN at $2\theta \approx 17°$. [c]Herman's orientation factor of PAN, calculated from the azimuthal scan of PAN (200) and (110) planes.

Meridional peak at $2\theta \approx 39°$ refers to the PAN (002) crystalline plane that is often used as an indicator of PAN polymer chain conformation and the periodic repeat distance along the fiber axis.[33−35] While the meridional peak location shifts toward lower 2θ values, PAN crystalline planes expand in the meridional direction,[33] which is analogous to a more extended polymer chain along the fiber axis, i.e., PAN molecules transform from helical to planar zigzag conformation. In this work, PAN fiber shows a meridional peak at 2θ = 39.25° at a draw ratio of 13. When lignin is incorporated in the fiber, the meridional peak location shifts to a higher 2θ value of 39.35°, indicating a shorter PAN crystalline plane along fiber axis compared to PAN fiber. This result shows that lignin molecules also affect the periodicity development in meridional direction.

Effects of CNT on Polymer Packing and Orientation. Previous studies show that CNT incorporation in PAN gel-spun fibers can promote PAN planar zigzag conformation.[36,37] In this study, a similar effect was observed as the merdional peak in PAN/lignin fiber at 39.35° shifted to 39.13° in the PAN/lignin/CNT fiber. This indicates that CNT can still promote a planar zigzag conformation of PAN in the presence of lignin. Interestingly, when PAN/lignin/CNT fiber shows more extended (planar zigzag) conformation, PAN polymer orientation and *d*-spacing values at $2\theta \approx 17°$ and $2\theta \approx 30°$ in both draw ratio samples are reduced. The decreased *d*-spacings along with the lower PAN orientation suggest that PAN, lignin, and CNT might be more tightly packed when lignin molecules "squeeze" the PAN crystalline region against CNT in fiber and thus affect the PAN polymer orientation. On the basis of the experimental data, the proposed schematics of the molecular packing in the three fully drawn fibers are shown in Figure 3.

Effect of Lignin and CNT on Mechanical Properties of Composite Fibers. The tensile properties of the precursor fibers (DR = 13) are reported in Table 2. PAN fiber shows a higher tensile modulus than PAN/lignin and PAN/lignin/CNT fibers, owing to better PAN orientation in the former case. Elongation at break of PAN, PAN/lignin, and PAN/lignin/CNT fibers are 8.1%, 7.1%, and 8.7%, respectively.

Results of the dynamic mechanical analysis are shown in Figure 4. Among PAN, PAN/lignin, and PAN/lignin/CNT fibers, PAN fiber exhibits the highest storage modulus. With the addition of CNT, PAN/lignin/CNT fiber shows a higher storage modulus than PAN/lignin fiber over the entire temperature range. The peak of the tan δ plot is referred to as the β_c relaxation temperature that relates to the PAN polymer chain motion in the paracrystalline region.[38] PAN precursor fiber shows a tan δ peak at 80.3 °C, while β_c relaxation in the PAN/lignin fiber shows a higher tan δ magnitude, broader range, and shifts to lower temperature (76.9 °C). The lower β_c transition temperature and broadened

DOI: 10.1021/acssuschemeng.5b00562
ACS Sustainable Chem. Eng. 2015, 3, 1943−1954

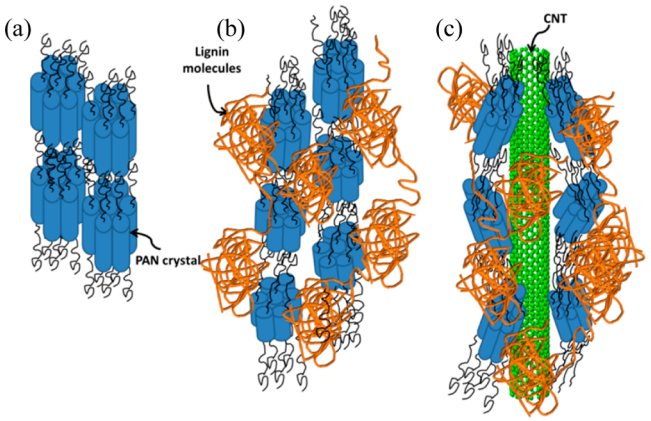

Figure 3. Schematics of (a) PAN, (b) PAN/lignin, showing a reduced PAN crystalline region, and (c) PAN/lignin/CNT, showing PAN crystal being squeezed by lignin and CNT.

Table 2. Mechanical Properties of Precursor Fibers at DR = 13

draw ratio =13	PAN	PAN/lignin	PAN/lignin/CNT
diameter (μm)	17.5 ± 1	18.5 ± 2.5	17.1 ± 0.3
tensile strength (MPa)	879 ± 65	742 ± 90	719 ± 45
tensile modulus (GPa)	19.9 ± 0.4	17.2 ± 1	17.7 ± 0.5
strain to failure (%)	8.1 ± 0.6	7.1 ± 0.6	8.7 ± 0.5

tan δ peak of the PAN/lignin fiber, as compared to the PAN fiber, imply that the molecular motion in the PAN/lignin fiber is less restricted. In other words, there is more free volume created by the presence of lignin molecules in PAN. A higher tan δ magnitude also suggests that the PAN polymer in the PAN/lignin fiber has more helical sequences as compared to the PAN fiber.[38] This is in agreement with the WAXD results discussed above. The PAN/lignin/CNT fiber shows a lower tan δ magnitude, narrower temperature range for the peak, and a higher β_c relaxation temperature (81.4 °C) than the PAN/lignin fiber. The lower magnitude and narrowing tan δ peak suggest a more tightly packed structure between the polymer and CNT that limits polymer mobility.[39−41]

Infrared spectra of lignin powder, as well as PAN and PAN/lignin fibers, are reported in Figure 5a. In lignin, the 1720 and 1050 cm^{-1} peaks correspond to the ketone-like structure. The sharp peaks from 1426 to 1510 cm^{-1} and the peak around 1600 cm^{-1} are due to C−C═C stretching in the aromatic rings, which are pervasive within monolignol units. The peaks from 1200 to 1050 cm^{-1} are attributed to the C−O stretching in

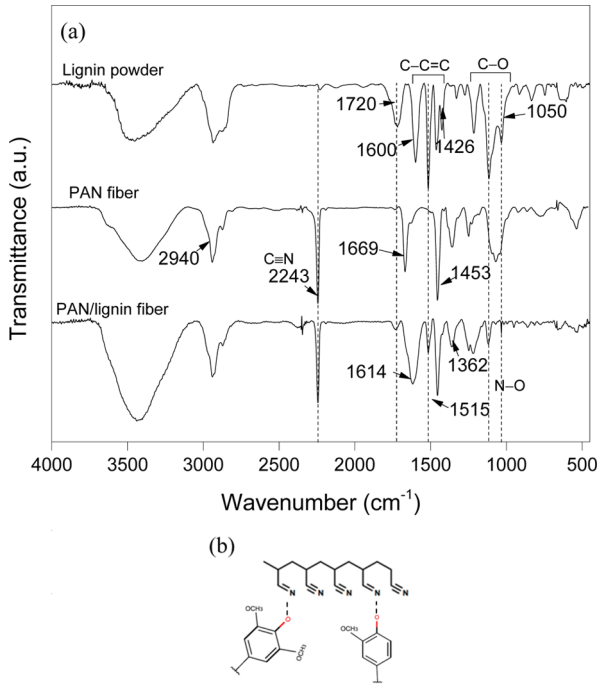

Figure 5. FTIR spectra (a) of lignin powder, PAN fiber (DR = 13), and PAN/lignin fiber (DR = 13) and (b) possible lignin/PAN interaction.

lignin alcohols. For PAN fiber, peaks at 1374, 1453, and 2940 cm^{-1} are assigned to CH_2 in the PAN backbone,[42] and the sharp peak at 2243 cm^{-1} belongs to the C≡N bond of PAN. For the PAN/lignin composite fiber, C−O and C−C═C stretching for aromatic rings are still observed in the spectrum. However, peaks of the ketone-like structure at 1720 and 1050 cm^{-1} are diminished significantly as compared to lignin spectra. This substantially decreased intensity for the lignin carbonyl peaks suggest this as the potential cite for interaction with the PAN nitrile group. The peaks at 1515 and 1362 cm^{-1} in the PAN/lignin fiber can be attributed to N−O stretching. Although these peaks were observed in previous PAN/lignin studies,[10,11] they were not discussed. The PAN/lignin fiber spectrum exhibited a slightly lower maginitude of the C≡N peak at 2243 cm^{-1} as compared to the PAN fiber and can be attributed to the reduced number of C≡N bonds in the blend fiber as compared to the control PAN fiber. The potential interaction between PAN and lignin is shown in Figure 5b, suggesting that some of the C≡N peak gets converted to C═

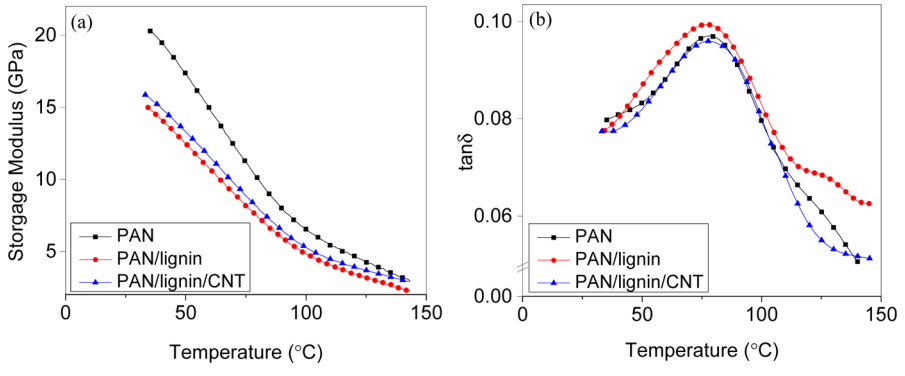

Figure 4. (a) Storage modulus and (b) tan δ plot vs temperature of precursor fibers (DR = 13) at 1 Hz.

DOI: 10.1021/acssuschemeng.5b00562
ACS Sustainable Chem. Eng. 2015, 3, 1943−1954

N and forms a N−O bond. The broadening of the peak at 1614 cm^{-1}, which can be attributed to the formation of the C═N bond, results from PAN interaction with lignin. The appearance of N−O peaks at 1515 and 1362 cm^{-1}, the diminishing of ketone peaks at 1720 and 1050 cm^{-1}, and somewhat lower C≡N peak magnitude at 2243 cm^{-1}, along with broadening of the 1614 cm^{-1} peak are thought to be the essential hints of PAN/lignin bond formation at PAN nitrile sites (Figure 5b).

Effect of Lignin and CNT on Stabilization Behavior of Composite Fibers. DSC analysis is performed on the precursor fibers in air environment, and the thermograms of the precursor fibers are shown in Figure 6. All precursor fibers

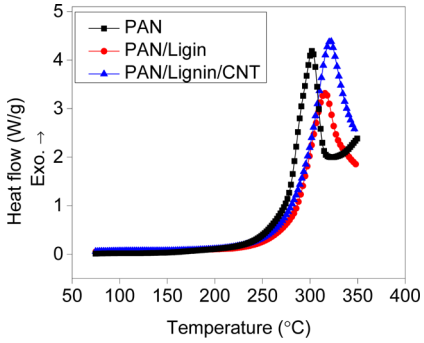

Figure 6. DSC thermograms for PAN fiber, PAN/lignin fiber, and PAN/lignin/CNT fiber (All DR = 13) at heating rate of 5 °C/min with air purging rate of 50 mL/min.

are heated from 50 to 350 °C at a heating rate of 5 °C/min. Exothermic peaks are observed during stabilization, and the heat of stabilization values are listed in Table 3. According to

Table 3. DSC Results of Precursor Fibers

precursor fibers	$\Delta H_{stabilization}$ (J/g)	fwhm (°C)
PAN	942	17.3
PAN/lignin	748	24.7
PAN/lignin/CNT	1189	25.2

the DSC thermograms, all fibers show a single exothermic peak, which formed by multiple stabilization reactions and free radical cyclization reaction.[43] The DSC curve of the PAN fiber shows a higher heat flow peak magnitude compared to the PAN/lignin DSC curve. This suggests that lignin can avoid excessive heat eruption during PAN stabilization, which is similar to the effect of acid-containing comonomers on PAN fibers.[44,45] Additionally, both PAN/lignin and PAN/lignin/CNT fibers show broader exothermic peaks as compared to PAN fibers. These observations suggest that lignin can potentially expedite the PAN fiber stabilization process.

Fiber shrinkage during the stabilization reactions is monitored through TMA under an applied stress of 10 MPa at a heating rate of 0.5 °C/min from room temperature to 280 °C followed by holding at 280 °C for 150 min. The temperature profile and fiber strain during heating are shown in Figure 7. Under these conditions, the ultimate thermal shrinkage of PAN, PAN/lignin, and PAN/lignin/CNT fibers are 20.3%, 21.2% and 13.0%, respectively. This data unequivocally shows that the presence of CNTs significantly reduces thermal shrinkage during stabilization. Previous studies show that the fiber shrinkage can be due to entropic relaxation (100−175 °C range), which allows the oriented amorphous

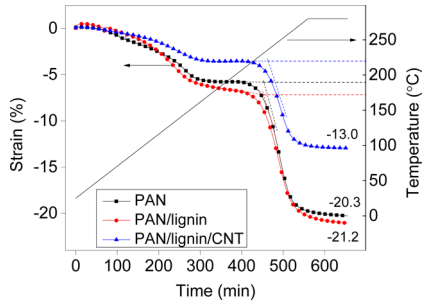

Figure 7. Fiber strain during TMA with corresponding temperature profile.

polymer phase to recoil, and due to chemical reaction (at above 175 °C) resulting from ladder structure formation.[37,46] The current TMA data shows that the PAN/lignin fiber shows earlier onset of polymer recoiling than the PAN fiber. This suggests that the incorporation of lignin can promote the entropic relaxation of polymer. PAN/lignin/CNT fiber, on the other hand, shows a much slower onset for entropic relaxation than the other two fibers. Previous studies have shown that the presence of CNTs can reduce thermal shrinkage in PAN.[37,39] This agrees with the current observations. The chemical reaction stage (above 175 °C) in Figure 7 corresponds to the cyclization of PAN molecules.[47] TMA results show that PAN/lignin fiber has earlier onset of the reaction than PAN and PAN/lignin/CNT fibers. Interestingly, this result correlates with the heat of stabilization ($\Delta H_{stabilization}$) observed from the DSC, where PAN/lignin fiber exhibits lower $\Delta H_{stabilization}$ than PAN fiber and PAN/lignin/CNT fiber. These findings imply that the incorporation of lignin can potentially promote the PAN cyclization during stabilization process, while the incorporation of CNT appears to delay this process.

Fiber Stabilization and Carbonization. Precursor fibers are stabilized under a stress of 22 MPa in the oxidative environment using a tube furnace. The fiber stabilization temperature profile is shown in Figure 8. During stabilization,

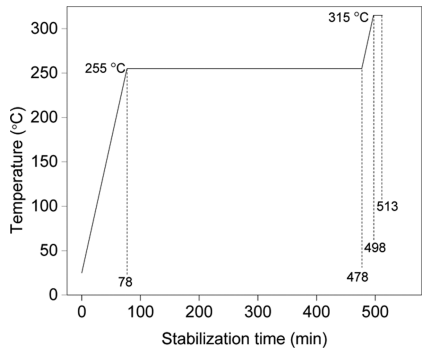

Figure 8. Stabilization temperature profile showing temperature stages and residence time with a constant heating rate of 3 °C per minute. Air flow rate is 50 standard cubic feet per hour (SCFH).

PAN is known to undergo cyclization, oxidation, and dehydrogenation.[44,47−49] Stabilization for lignin is generally considered to be initiated by the homolytic cleavage of alkyl-aryl ether linkage and leads to further lignin units rearrangement and cross-linking.[50−53] FTIR spectra of stabilized PAN and PAN/lignin fibers are shown in Figure 9. After oxidative stabilization, the PAN fiber shows a diminishing C≡N structure at 2244 cm^{-1}.[54] Additionally, the appearance of

DOI: 10.1021/acssuschemeng.5b00562
ACS Sustainable Chem. Eng. 2015, 3, 1943−1954

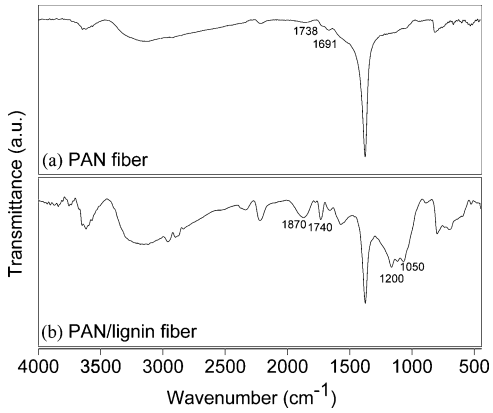

Figure 9. FTIR spectra of (a) PAN and (b) PAN/lignin fibers stabilized under conditions described in Figure 8.

peak shoulders at 1691 and 1738 cm^{-1} corrspond to the C═O stretching of carbonyls. Stabilized PAN/lignin fiber shows clear 1050−1200 cm^{-1} peaks, which are due to C−O stretching with possible overlap with a C−N peak. Similar to stabilized PAN fiber, the peak at 1740 cm^{-1} is assigned to the C═O stretching in carbonyls for the stabilized PAN/lignin fiber.[51] A new peak is observed about 1870 cm^{-1} in the stabilized PAN/lignin fiber. Previous XPS studies used this peak to identify anhydride linkage formation from the cross-linking of stabilized lignins.[51,52] Addtiontionally, small peaks between 2860−2970 cm^{-1} in the stabilized PAN/lignin fiber spectra represent C−H stretching from aromatic and aliphatic carbons, which are attributed to lignin units after stabilization.[51] The differences between stabilized PAN and PAN/lignin fiber spectra show evidence of both PAN and lignin stabilization reactions.

Integrated WAXD scans of precursor, stabilized, and carbon fibers along with the WAXD patterns of the stabilized and carbon fibers are shown in Figure 10. All integrated scans of precursor fibers show a distinct PAN peak at $2\theta \approx 17°$, which diminishes upon stabilization. The peak at $2\theta \approx 26°$ in stabilized and carbonized fibers is due to the formation of a carbon ladder structure. Structural parameters of stabilized fibers are shown in Table 4. CNT-incorporated stabilized fiber shows a relatively large crystal size (1.4 vs 1.1 and 1.0 nm in PAN- and PAN/lignin-based fibers, respectively) corresponding to the $2\theta \approx 26°$ peak, suggesting that CNTs promote the development of the cyclized ladder structure in the vicinity of CNT. Compared with the PAN stabilized fiber, PAN/lignin shows slightly lower crystal size corresponding to the peak at $2\theta \approx 43°$, indicating that the formation of the cyclized ladder

Table 4. Structural Parameters of Stabilized Fibers

stabilized fibers	PAN	PAN/lignin	PAN/lignin/CNT
$L2\theta \approx 26°$[a] (nm)	1.1	1.0	1.4
$L2\theta \approx 43°$[b] (nm)	1.4	1.2	1.6
f_{ladder}[c]	0.66	0.65	0.65
d-spacing ($2\theta \approx 26°$) (Å)	3.43	3.48	3.40

[a]Crystal size of ladder structure at $2\theta \approx 26°$. [b]Crystal size from meridional scan at $2\theta \approx 43°$. [c]Orientation of ladder structure of stabilized fibers.

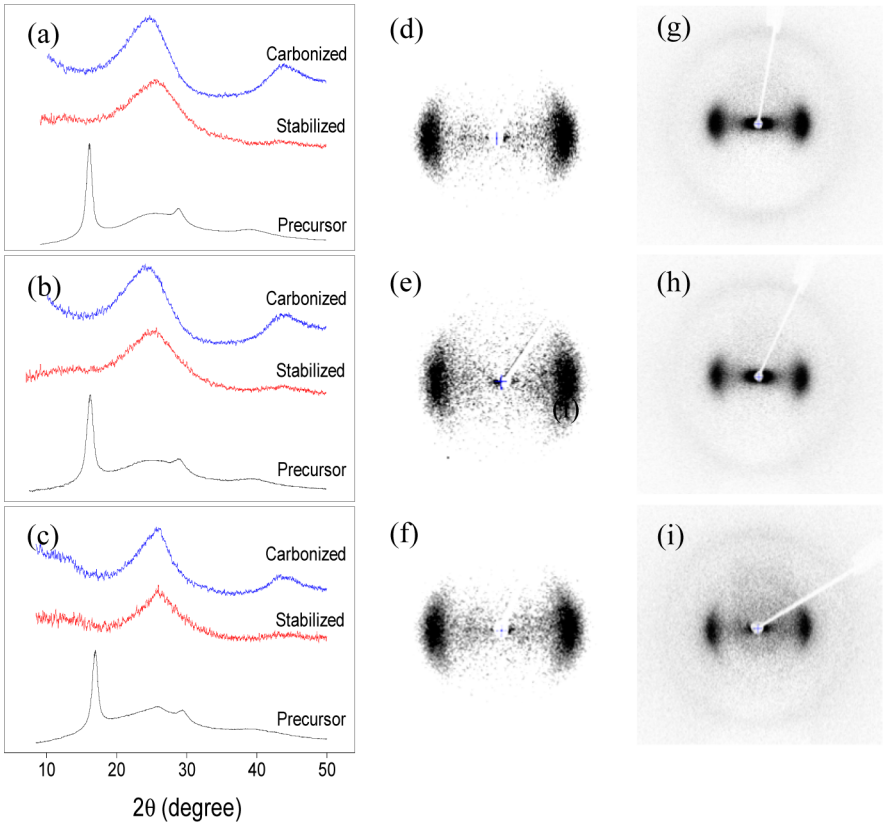

Figure 10. Integrated scans of precursors, stabilized, and carbon fibers for (a) PAN, (b) PAN/lignin, and (c) PAN/lignin/CNT fibers with the corresponding WAXD patterns of stabilized (d) PAN, (e) PAN/lignin, and (f) PAN/lignin/CNT fibers and carbonized (1000 °C) (g) PAN, (h) PAN/lignin, and (i) PAN/lignin/CNT fibers.

DOI: 10.1021/acssuschemeng.5b00562
ACS Sustainable Chem. Eng. 2015, 3, 1943−1954

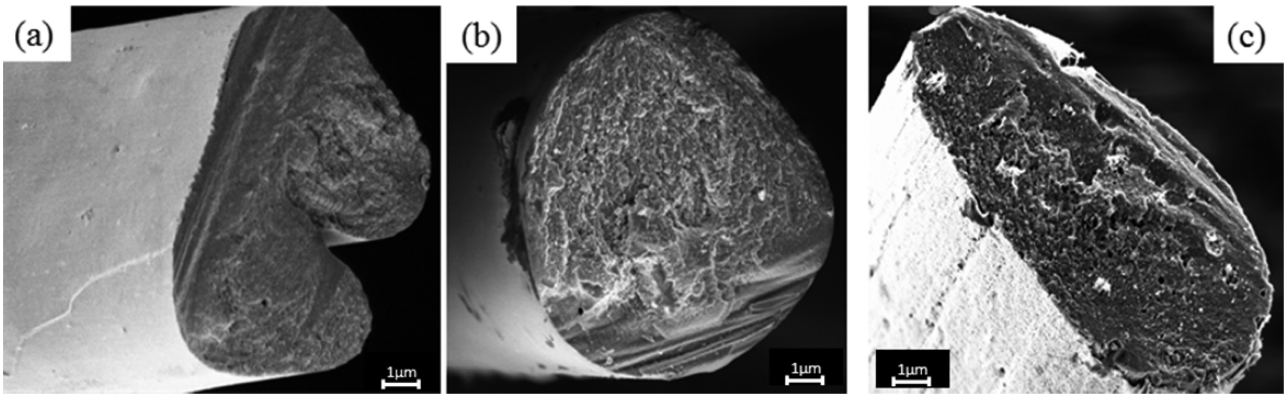

Figure 11. SEM images of carbon fiber cross sections of (a) PAN, (b) PAN/lignin, and (c) PAN/lignin/CNT carbonized at 1100 °C.

Table 5. Structural Parameters and Tensile Properties of Carbon Fibers

carbon fiber structural parameters						
carbonize Temp (°C)	1000 °C			1100 °C		
carbon fiber	PAN	PAN/lignin	PAN/lignin/CNT	PAN	PAN/lignin	PAN/lignin/CNT
L002[a] (nm)	1.3	1.3	1.6	1.3	1.4	1.8
L10[b] (nm)	1.5	1.5	1.7	2.3	2.0	1.9
f_{002}[c]	0.80	0.78	0.75	0.81	0.80	0.77
Z[d]	34.4	34.9	35.5	32.7	32.8	33.2
d-spacing $_{(002)}$ (Å)	3.48	3.53	3.51	3.51	3.52	3.49
carbon fiber tensile properties						
diameter (μm)	10.5 ± 0.6	11.0 ± 1.1	9.0 ± 0.3	11.0 ± 0.7	11.0 ± 1.1	8.8 ± 0.3
strength (GPa)	1.54 ± 0.6	1.37 ± 0.2	1.29 ± 0.2	1.60 ± 0.3	1.72 ± 0.2	1.40 ± 0.2
modulus[e] (GPa)	193 ± 12	194 ± 8	181 ± 5	223 ± 4	230 ± 7	200 ± 7
elong. at break (%)	0.83 ± 0.2	0.72 ± 0.1	0.72 ± 0.1	0.70 ± 0.1	0.80 ± 0.1	0.71 ± 0.1

[a]Crystal size of (002) plane. [b]Crystal size of (10) plane. [c]Orientation of (002) structure of carbon fibers. [d]Full width half-maximum (fwhm) (in degree) from azimuthal scans of (002) planes. [e]Modulus values have not been corrected for instrumental compliance.

structure along the fiber axis might be disturbed by the incorporation of lignin. In addition to larger crystal sizes, stabilized fiber containing CNT has a smaller ladder structure d-spacing of 3.40 Å, as compared to 3.43 and 3.48 Å in PAN and PAN/lignin fibers, respectively. Similar observations are found in previous studies on PAN/CNT fibers.[55,56]

Stabilized fibers are carbonized under inert environment at a constant heating rate of 5 °C/min to 1000 and 1100 °C. No fusing of stabilized or carbonized fibers is observed, indicating proper heating rate is applied during each process for lignin incorporated fibers.[9,57] After carbonization, the ladder structure from stabilization is then transformed into carbonized turbostratic carbon structure.[56] SEM images of the carbon fiber cross sections are shown in Figure 11. Under the identical stabilization and carbonization conditions, PAN and PAN/lignin carbon fibers show no voids in the fiber cross sections, while the PAN/lignin/CNT carbon fiber exhibits more observable voids which would be detrimental for mechanical properties. The void formation caused by CNT was not noted in previous PAN/CNT batch processed carbon fiber studies.[19,37,47,56,58] However, in a recent PAN/CNT carbon fiber study, void formation was noted, and the presence of these voids was attributed to nonuniform CNT length, and CNT bundling.[24]

The structural parameters and mechanical properties of carbonized fibers are summarized in Table 5. At both carbonization temperatures (1000 and 1100 °C), PAN/lignin/CNT fibers show relatively low orientation as compared to PAN and PAN/lignin fibers; this can result from lower PAN orientation in CNT-containing precursor fibers. The lower orientation along with more voids in the PAN/lignin/CNT carbon fiber results in lower tensile properties,[59] as compared to the PAN and PAN/lignin fibers. All carbon fibers show improvements in tensile strength and tensile modulus with a simultaneous increase in crystal size for the (10) plane with increasing carbonization temperatures. When carbonized at 1000 °C, PAN carbon fiber shows tensile strength, tensile modulus, and elongation at break of 1.54 GPa, 193 GPa, and 0.83%, respectively. When carbonized at 1100 °C, the tensile modulus of the PAN fiber is increased to 223 GPa, with a slightly decreased elongation at break of 0.70% and a relatively unchanged tensile strength of 1.60 GPa. Carbonized at 1000 °C with identical conditions, the PAN/lignin fiber shows comparable tensile modulus (194 GPa) but lower tensile strength (1.37 GPa) and elongation at break (0.72%). Interestingly, when carbonized at 1100 °C, the PAN/lignin carbon fiber exhibits noticeable improvement in tensile strength (1.72 GPa) and tensile modulus (230 GPa), while elongation at break remains intact (0.80%).

Raman spectra of carbon fibers are shown in Figure 12. The Raman D-band (at ~1330 cm^{-1}) is attributed to the structural disorder, and the G-band (at ~1560 cm^{-1}) is assigned to the graphitic planes. The fwhm of both D and G bands along with the intensity ratio are normally used to characterize carbon materials[60−64] and to understand the carbonization mechanism of wood materials.[65,66] For example, the amorphization

DOI: 10.1021/acssuschemeng.5b00562
ACS Sustainable Chem. Eng. 2015, 3, 1943−1954

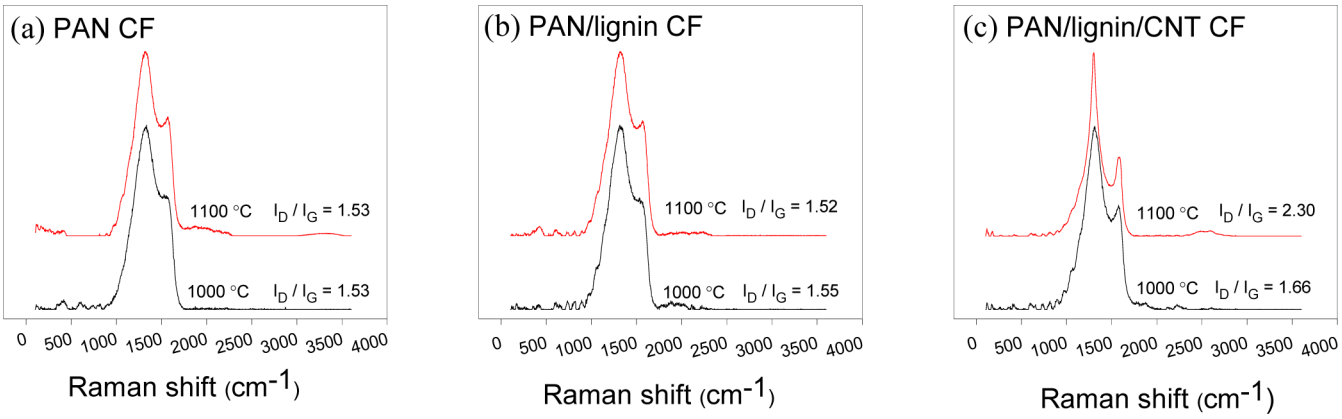

Figure 12. Raman spectra of fibers (a) PAN, (b) PAN/lignin, and (c) PAN/lignin/CNT carbonized at 1000 and 1100 °C.

trajectory can also be used to analyze carbonization behaviors by describing the transformation of neat graphite to nanocrystalline graphite and further to sp^3 amorphous carbon. As carbon transforms along this amorphization trajectory, I_D/I_G will first increase due to defects in the graphite structure and then decrease during nanocrystalline graphite formation. This is followed by a further decrease in I_D/I_G owing to the formation of amorphous carbon.[61,62] In Raman spectroscopy studies on carbon materials, the Tuinstra−Koenig law was often employed to estimate crystal size by correlation with intensity ratio I_D/I_G.[67] However, studies have shown that the Tuinstra−Koenig correlation is not applicable when crystal sizes are below 2 nm, as it results in significant discrepancies.[68,69] In this study, we note that the crystal sizes obtained from WAXD in Table 5 were mostly below 2 nm. Therefore, Raman spectral features in the current study have not been used for crystal size determination. Raman spectroscopy and amorphization trajectory were used to study the electrospun kraft lignin and PAN fibrous materials carbonized at 600, 800, and 1000 °C by Dallmeyer et al.[70] While PAN is considered as a semicrystalline material, carbonization between 600 and 1000 °C induces the nanocrystalline carbon formation that yields decreasing I_D/I_G values with increasing carbonization temperature. Lignin, in contrast, started with a much more amorphous state, can transform to nanocrystalline carbon from nucleation and growth of disordered aromatic rings. PAN and lignin were then reported to undergo distinct stages of carbonization between 600 to 1000 °C.[70]

When carbonized at 1000 °C, all carbon fibers show obvious D-band peaks. PAN and PAN/lignin carbon fibers show G-band peaks as shoulders while PAN/lignin/CNT exhibits a more resolved G-band peak (Figure 12). When carbonization temperature is increased to 1100 °C, further developments in the graphitic G-band for all the fibers are observed. Surprisingly, although G-band peaks seem to be more significant when carbonized at 1100 °C, PAN and PAN/lignin carbon fibers show no significant changes in I_D/I_G values (Figure 12a, b) while PAN/lignin/CNT fiber shows noticeably increased intensity peak ratio from 1.66 to 2.30 in going from 1000 to 1100 °C (Figure 12c). This implies that the incorporation of CNT might induce the transformation from amorphous carbon to nanocrystalline graphite when carbonized from 1000 to 1100 °C, as the development of the D-peak can indicate the ordering of amorphous carbons.[62]

The D and G band fwhm of the carbon fibers are shown in Figures 13 and 14, respectively. In general, D-band fwhm values of carbonized wood materials are reported to decrease with increasing carbonization temperatures, indicating the ordering of polyaromatic carbons and the breakage of cross-linking between aliphatic carbons and small aromatic carbons.[66,70] For the lignin-incorporated carbon fibers in this work, a similar trend is observed (Figure 13). Both PAN/lignin and PAN/lignin/CNT fibers show a noticeable decrease in D-band fwhm, when carbonization temperature is increased. However, the D-band fwhm of PAN fiber does not exhibit significant change. This suggests that when incorporating lignin into PAN, reordering of polyaromatic stacks still occurs at elevated carbonization temperautres. Although both PAN/lignin and PAN/lignin/CNT fibers show a narrowing D-band fwhm, PAN/lignin/CNT exhibits a more significant change than the PAN/lignin fiber, suggesting that the presence of CNT promotes further reordering of the disordered aromatic rings in the carbon fiber.

G-band fwhm is often employed to characterize carbon crystallites. A narrower G-band fwhm implies a more ordered structure of carbon crystallites.[64,65,71] Although the G-band fwhm of carbon materials is expected to decrease at higher carbonization temperatures, Dallmeyer et al. reported an increasing G-band fwhm when lignin is carbonized from 600 to 1000 °C. This might be ascribed to an increase in the nonaromatic conjugated structure during polyaromatics reordering.[70] In Figure 14, PAN carbon fiber shows a decrease in the G-band fwhm from 1000 to 1100 °C, which can be attributed to a more refined structure at increased carbonization temperatures.[72] In contrast, the G-band fwhm of the PAN/lignin carbon fiber stays relatively unchanged when the carbonization temperature is increased from 1000 to 1100 °C. This unchanged G-band fwhm of PAN/lignin suggests that the breaking of cross-linking between the aliphatic and aromiatic carbons discussed above can offset the ordering of PAN crystalline carbons. This indicates that carbon crystallite refining and polyaromatic ordering are ongoing simultaneously in this temperature range. Interestingly, PAN/lignin/CNT shows a significant narrowing for both the G- and D-bands fwhm in going from 1000 to 1100 °C. This finding agrees with the reported crystallites ordering during carbonization when CNTs are embedded in the PAN nanofibers, where the G-band fwhm is found to decrease with increasing CNT concentration.[55]

DOI: 10.1021/acssuschemeng.5b00562
ACS Sustainable Chem. Eng. 2015, 3, 1943−1954

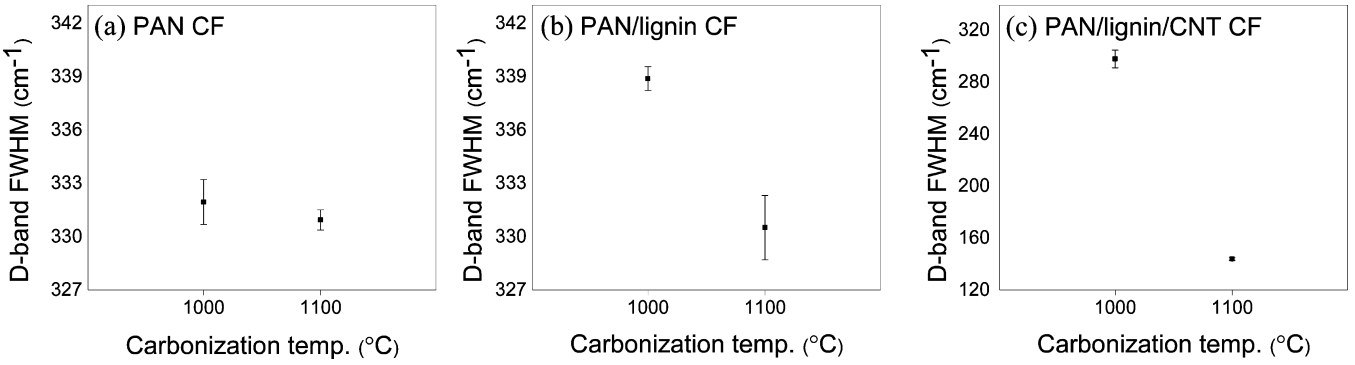

Figure 13. D-band fwhm when carbonized from 1000 to 1100 °C for (a) PAN, (b) PAN/lignin, and (c) PAN/lignin/CNT.

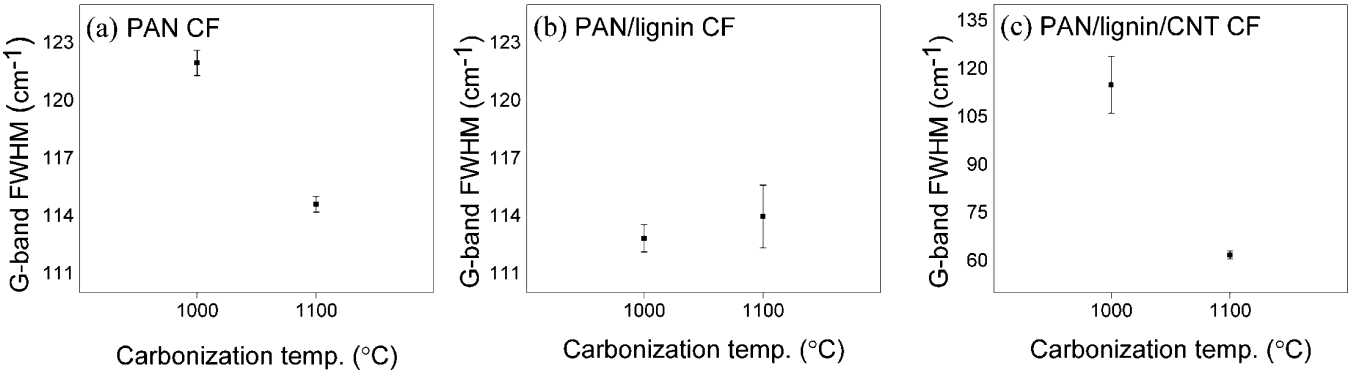

Figure 14. G-band fwhm when carbonized from 1000 to 1100 °C for (a) PAN, (b) PAN/lignin, and (c) PAN/lignin/CNT.

DISCUSSION AND CONCLUDING REMARKS

PAN, PAN/lignin (70/30 weight ratio), and PAN/lignin/CNT (70/30/3 weight ratio) precursor fibers have been successfully manufactured through gel-spinning. It is noted that while PAN fiber could be spun at a concentration of 14 g/dL, PAN/lignin and PAN/lignin/CNT fibers could be spun at a concentration of 20 and 25.75 g/dL, respectively. These significant differences in the spinning concentrations, along with differences in the spinning temperatures (as discussed in the Experimental Section), provided the first evidence of an interaction between these binary and ternary blend systems in DMAc. Subsequent studies on the precusrsor and carbon fibers provided further evidence of PAN/lignin and PAN/lignin/CNT interaction by spectroscopic (FTIR and Raman) and physio-mechanical methods (WAXD, DMA, DSC, TMA). These studies show that the incorporation of lignin affects PAN polymer chain packing, as well as the fiber stabilization and carbonization behavior. FTIR spectra shows the evidence of a specific interaction between lignin and PAN. DSC studies show that as compared to PAN, PAN/lignin fiber exhibits a broader exothermic peak of lower magnitude, while TMA exhibited an earlier onset of PAN cyclization. These studies suggest that lignin promotes PAN stabilization. In the presence of CNT, thermal shrinkage of the fiber is significantly reduced during stabilization. The conversion process of the precursor fibers to carbon fibers have been studied, and carbon fiber fabrication of all fibers is successfully achieved under identical conditions. Void-free carbon fibers have been made from gel-spun PAN/lignin precursor fibers, while other studies reported in the literature to date based on solution-spun PAN/lignin fibers all show significant voids in the final carbon fiber.[14,16,17,73] This comparison shows the advantage of the gel-spinning technique for making void-free carbon fibers from a PAN/lignin blend.

When carbonized at 1100 °C under identical conditions, the mechanical properties of the PAN/lignin carbon fiber is comparable to that of the PAN carbon fiber. By comparison, other studies in the literature to date show lower properties for the carbon fibers from PAN/lignin than from PAN. Therefore, it has been clearly demonstarted that by the gel-spinning process, lignin can be incorporated into PAN-based carbon fibers without compromising mechanical properties. Mechanical properties of the PAN/lignin carbon fiber in the current study already exceeds U.S. Department of Energy target mechanical properties for automotive composites (DOE target tensile strength is 1.75 GPa, and the target tensile modulus is 175 GPa). The properties achieved in the current study will be further improved for the following reasons: (a) Highest tensile strength carbon fibers are processed at a temperature in the range from 1400 to 1600 °C,[2,74] while the carbonization in the current study was only carried out at a maximum temperature of 1100 °C. (b) Fiber modulus almost linearly increases with increasing carbonization temperature.[2] (c) High strength and high modulus carbon fibers are always processed on continuous stabilization and carbonization lines, where fiber tension can be controlled to different levels in stepwise temperature zones and carbonization time in the high temperature range (500−1600 °C range) can be limited to few minutes. Therefore, when the gel-spun PAN/lignin fiber is carbonized on a continuous stabilization and carbonization line, where temperature and tension can be controlled in various stabilization and carbonization temperature zones, significant further improvements in tensile strength and modulus can be expected. While comparing the mechanical properties of the PAN/lignin carbon fibers in the current study to that of the Zoletk study, it should

DOI: 10.1021/acssuschemeng.5b00562
ACS Sustainable Chem. Eng. 2015, 3, 1943−1954

be noted that the fibers in the current study were processed in batch mode at a maximum temperature of 1100 °C (due to temperature limitation of the furnace). In the Zoltek study, carbonization temperature was not reported. However, based on the known parameters for achieving high strength carbon fibers, we presume that Zoltek fibers would have been carbonized somewhere in the 1400−1600 °C temperature range. We also note that the modulus in the current study has not been corrected for instrumental compliance, and with this correction, the carbon fiber modulus in the current study will be about 5−7% higher than the values given in Table 5.[75]

Continuous stabilization and carbonization of gel-spun PAN fiber has resulted in a new milestone in developing high strength and high modulus carbon fibers, where average tensile strength and tensile modulus based on standard test protocols were in the range from 5.5 to 5.8 GPa and 350 to 380 GPa, respectively.[76] At short gauge length tensile strength of gel-spun PAN-based carbon fiber was as high as 12 GPa.[76] This is a record tensile strength for a PAN-based carbon fiber at any gauge length. Thus, considering that there is no loss in the mechanical properties of the gel-spun PAN/lignin-based carbon fiber in the current study as compared to the gel-spun PAN-based carbon fiber, it can be expected that PAN/lignin-based carbon fiber can compete in properties with the best in class PAN-based carbon fibers with appropriate materials and process optimization.

In addition, due to the significantly lower cost of lignin as compared to PAN, PAN/lignin-based fibers will have lower cost than PAN-based carbon fibers along with higher production rate from the acclerated stabilization process with the incorporation of lignin. With lignin being a biorenewable product, PAN/lignin-based carbon fibers will be more sustainable than PAN-based carbon fiber, as PAN is currently derived from petroleum. In addition, due to the three-dimensional nature of the lignin molecule, PAN/lignin-based carbon fibers are expected to have good compressive strength. This is in contrast to the pitch-based carbon fibers, where pitch leads to highly graphitic two-dimensional structure and hence low compressive strength.[2,77]

With the incorporation of lignin, CNT, or both, the carbonization behavior of PAN is altered. When the carbonization temperature increases, PAN shows a narrowing G-band fwhm corresponding to lower structural disorder and a relatively unchanged D-band fwhm. PAN/lignin shows no significant change in G-band fwhm but a noticeably narrowing D-fwhm that is attributed to aliphatic and aromatic carbons reordering. The PAN/lignin/CNT carbon fiber shows significant reduction in both the G- and D-band fwhm, as compared to the PAN/lignin carbon fiber. This suggests that the presence of CNT can induce both structural reordering of PAN and aliphatic/aromatic carbon reordering during carbonization. Despite the enhanced order/crystal size, somewhat lower mechnical properties of PAN/lignin/CNT-based carbon fibers, as compared to PAN- and PAN/lignin-based carbon fibers, can be attributed to the presence of voids in the former fiber. The CNT diameter used in the current study, at 21.0 ± 3.1 nm, was significanly larger than the CNT diameter used in our previous studies, where CNT diameter was in the range from 1 to 12 nm.[19,24,56,78,79] The large CNT diameter in the current study may at least be partially responsible for the lower tensile strength of the PAN/lignin/CNT-based carbon fiber. On the other hand, the lower tensile modulus of the PAN/lignin/CNT-based carbon fiber as compared to the PAN- and PAN/lignin-based carbon fibers was a result of lower graphitic plane orientation in the former fiber (Table 5). Consequently, the question is this: Is there an advantage to the addition of CNT in PAN/lignin for making carbon fiber? In yet another recent study on PAN/CNT fiber, it has been shown that the addition of 0.5 to 1 wt % CNT in PAN results in about a 25% increase in axial electrical conductivity and up to a 100% increase in thermal conductivity of the PAN-based carbon fiber.[24] Similarly, PAN/lignin-based carbon fibers with enhanced electrical and thermal conductivities can be produced with the addition of CNT. The exact influence on mechanical properties, as well as on electrical and thermal conductivity of the PAN/lignin/CNT-based carbon will depend on CNT length, diameter, and perfection, as well as on CNT dispersion in the matrix. Interaction of CNT has been shown on PAN previously[19,24,39,58,79] and on the PAN/lignin blend in this study. Similarly, PAN/lignin fibers can also be processed with the addition of graphene nano ribbons, as well as graphene nano ribbons.[80]

AUTHOR INFORMATION

Corresponding Author

*Phone: +1-404-894-7550. Fax +1-404-894-8780. E-mail: Satish.Kumar@mse.gatech.edu.

Notes

The authors declare no competing financial interest.

ACKNOWLEDGMENTS

This work is supported by the Renewable Bioproducts Institute at Georgia Institute of Technology and a grant from the Air Force Office of Scientific Research (FA 9550-14-1-0194).

REFERENCES

(1) Huang, X. S. Fabrication and Properties of Carbon Fibers. *Materials* **2009**, *2* (4), 2369−2403.

(2) Minus, M. L.; Kumar, S. The Processing, Properties, and Structure of Carbon Fibers. *JOM* **2005**, *57* (2), 52−58.

(3) Liu, Y.; Kumar, S. Recent Progress in Fabrication, Structure, and Properties of Carbon Fibers. *Polym. Rev.* **2012**, *52* (3−4), 234−258.

(4) Calvo-Flores, F. G.; Dobado, J. A. Lignin as Renewable Raw Material. *ChemSusChem* **2010**, *3* (11), 1227−1235.

(5) Baker, D. A.; Rials, T. G. Recent Advances in Low-Cost Carbon Fiber Manufacture from Lignin. *J. Appl. Polym. Sci.* **2013**, *130* (2), 713−728.

(6) Sudo, K.; Shimizu, K. A New Carbon Fiber from Lignin. *J. Appl. Polym. Sci.* **1992**, *44* (1), 127.

(7) Frank, E.; Hermanutz, F.; Buchmeiser, M. R. Carbon Fibers: Precursors, Manufacturing, and Properties. *Macromol. Mater. Eng.* **2012**, *297* (6), 493−501.

(8) Kubo, S.; Kadla, J. F. Lignin-based Carbon Fibers: Effect of Synthetic Polymer Blending on Fiber Properties. *J. Polym. Environ.* **2005**, *13* (2), 97−105.

(9) Kadla, J. F.; Kubo, S.; Venditti, R. A.; Gilbert, R. D.; Compere, A. L.; Griffith, W. Lignin-based Carbon Fibers for Composite Fiber Applications. *Carbon* **2002**, *40* (15), 2913.

(10) Maradur, S. P.; Kim, B. H.; Yang, K. S.; Kim, C. H.; Kim, S. Y.; Kim, W. C. Preparation of Carbon Fibers from a Lignin Copolymer with Polyacrylonitrile. *Synth. Met.* **2012**, *162* (5−6), 453−459.

(11) Seydibeyoğlu, M. Ö. A Novel Partially Biobased PAN-Lignin Blend as a Potential Carbon Fiber Precursor. *J. Biomed. Biotechnol.* **2012**, *2012*, 1−8.

(12) Alexy, P.; Košíková, B.; Podstránska, G. The Effect of Blending Lignin with Polyethylene and Polypropylene on Physical Properties. *Polymer* **2000**, *41* (13), 4901−4908.

DOI: 10.1021/acssuschemeng.5b00562
ACS Sustainable Chem. Eng. 2015, 3, 1943−1954

(13) Thunga, M.; Chen, K.; Grewell, D.; Kessler, M. R. Bio-renewable Precursor Fibers from Lignin/Polylactide Blends for Conversion to Carbon Fibers. *Carbon* **2014**, *68* (0), 159−166.
(14) Husman, G. In *Development and Commercialization of a Novel Low-Cost Carbon Fiber*; Presentation at 2012 DOE Hydrogen and Fuel Cells Program and Vehicle Technologies Program Annual Merit Review and Peer Evaluation Meeting, 2012.
(15) Bissett, P. J.; Herriott, C. W. Lignin/Polyacrylonitrile-Containing Dopes, Fibers, and Methods of Making Same. U.S. Patent 2012/0003471, 2012.
(16) Husman, G. In *Development and Commercialization of a Novel Low-Cost Carbon Fiber*; Presentation at 2014 DOE Hydrogen and Fuel Cells Program and Vehicle Technologies Office Annual Merit Review and Peer Evaluation Meeting, 2014.
(17) Dong, X.; Lu, C.; Zhou, P.; Zhang, S.; Wang, L.; Li, D. Polyacrylonitrile/lignin Sulfonate Blend Fiber for Low-cost Carbon Fiber. *RSC Adv.* **2015**, *5* (53), 42259−42265.
(18) Ragauskas, A. J.; Beckham, G. T.; Biddy, M. J.; Chandra, R.; Chen, F.; Davis, M. F.; Davison, B. H.; Dixon, R. A.; Gilna, P.; Keller, M.; Langan, P.; Naskar, A. K.; Saddler, J. N.; Tschaplinski, T. J.; Tuskan, G. A.; Wyman, C. E. Lignin Valorization: Improving Lignin Processing in the Biorefinery. *Science* **2014**, *344* (6185), 1246843.
(19) Chae, H. G.; Choi, Y. H.; Minus, M. L.; Kumar, S. Carbon Nanotube Reinforced Small Diameter Polyacrylonitrile Based Carbon Fiber. *Compos. Sci. Technol.* **2009**, *69* (3−4), 406−413.
(20) Chae, H. G.; Kumar, S. Making Strong Fibers. *Science* **2008**, *319* (5865), 908.
(21) Chae, H. G. Polyacrylonitrile/Carbon Nanotube Composite Fibers: Reinforcement Efficiency and Carbonization Studies. Ph.D Thesis. Georgia Institute of Technology, Atlanta, GA, 2008.
(22) Chien, A.; Gulgunje, P. V.; Chae, H. G.; Joshi, A. S.; Moon, J.; Feng, B.; Peterson, G. P.; Kumar, S. Functional polymer−polymer/carbon nanotube bi-component fibers. *Polymer* **2013**, *54* (22), 6210−6217.
(23) Liu, Y.; Kumar, S. Polymer/Carbon Nanotube Nano Composite Fibers−A Review. *ACS Appl. Mater. Interfaces* **2014**, *6* (9), 6069−6087.
(24) Newcomb, B. A.; Giannuzzi, L. A.; Lyons, K. M.; Gulgunje, P. V.; Gupta, K.; Liu, Y.; Kamath, M. G.; McDonald, K.; Moon, J.; Feng, B.; Peterson, G. P.; Chae, H. G.; Kumar, S. High Resolution Transmission Electron Microscopy Study on Polyacrylonitrile/Carbon Nanotube Based Carbon Fibers and the Effect of Structure Development on the Thermal and Electrical Conductivities. *Carbon* **2015**, *93*, 502−514.
(25) Baker, F. S.; Baker, D. A.; Menchhofer, P. A. Carbon Nanotube (CNT)-Enhanced Precursor for Carbon Fiber Production and Method of Making a CNT-enhanced Continous Lignin Fiber. U.S. Patent 2011/0285049 A1, 2011.
(26) Teng, N.; Dallmeyer, I.; Kadla, J. F. Incorporation of Multiwalled Carbon Nanotubes into Electrospun Softwood Kraft Lignin-Based Fibers. *J. Wood Chem. Technol.* **2013**, *33* (4), 299−316.
(27) Teng, N.; Dallmeyer, I.; Kadla, J. F. Effect of Softwood Kraft Lignin Fractionation on the Dispersion of Multiwalled Carbon Nanotubes. *Ind. Eng. Chem. Res.* **2013**, *52* (19), 6311−6317.
(28) Sahoo, S.; Seydibeyoğlu, M. Ö.; Mohanty, A. K.; Misra, M. Characterization of Industrial Lignins for Their Utilization in Future Value Added Applications. *Biomass Bioenergy* **2011**, *35* (10), 4230−4237.
(29) Allen, R. A.; Ward, I. M.; Bashir, Z. The Variation of the d-Spacings with Stress in the Hexagonal Polymorph of Polyacrylonitrile. *Polymer* **1994**, *35* (19), 4035−4040.
(30) Bashir, Z. A Critical Review of the Stabilisation of Polyacrylonitrile. *Carbon* **1991**, *29* (8), 1081−1090.
(31) Bashir, Z. Co-crystallization of Solvents with Polymers: the X-ray Diffraction Behavior of Solvent-containing and Solvent-free Polyacrylonitrile. *J. Polym. Sci., Part B: Polym. Phys.* **1994**, *32* (6), 1115−1128.
(32) Sokół, M.; Grobelny, J.; Turska, E. Investigation of Structural Changes of Polyacrylonitrile on Swelling. Wide-Angle X-ray Scattering Study. *Polymer* **1987**, *28* (5), 843−846.
(33) Gong, Y.; Du, R.; Mo, G.; Xing, X.; Lü, C.; Wu, Z. In-situ Microstructural Changes of Polyacrylonitrile Based Fibers with Stretching Deformation. *Polymer* **2014**, *55* (16), 4270−4280.
(34) Sawai, D.; Yamane, A.; Kameda, T.; Kanamoto, T.; Ito, M.; Yamazaki, H.; Hisatani, K. Uniaxial Drawing of Isotactic Poly(acrylonitrile): Development of Oriented Structure and Tensile Properties. *Macromolecules* **1999**, *32* (17), 5622−5630.
(35) Yamane, A.; Sawai, D.; Kameda, T.; Kanamoto, T.; Ito, M.; Porter, R. S. Development of High Ductility and Tensile Properties upon Two-Stage Draw of Ultrahigh Molecular Weight Poly(acrylonitrile). *Macromolecules* **1997**, *30* (14), 4170−4178.
(36) Wang, W.; Murthy, N. S.; Chae, H. G.; Kumar, S. Structural Changes During Deformation in Carbon Nanotube-reinforced Polyacrylonitrile Fibers. *Polymer* **2008**, *49* (8), 2133−2145.
(37) Liu, Y.; Chae, H. G.; Kumar, S. Gel-spun Carbon Nanotubes/Polyacrylonitrile Composite Fibers. Part I: Effect of Carbon Nanotubes on Stabilization. *Carbon* **2011**, *49*, 4466−4476.
(38) Sawai, D.; Kanamoto, T.; Yamazaki, H.; Hisatani, K. Dynamic Mechanical Relaxations in Poly(acrylonitrile) with Different Stereoregularities. *Macromolecules* **2004**, *37* (8), 2839−2846.
(39) Chae, H. G.; Sreekumar, T. V.; Uchida, T.; Kumar, S. A Comparison of Reinforcement Efficiency of Various Types of Carbon Nanotubes in Polyacrylonitrile Fiber. *Polymer* **2005**, *46* (24), 10925−10935.
(40) Arrighi, V.; McEwen, I. J.; Qian, H.; Serrano Prieto, M. B. The Glass Transition and Interfacial Layer in Styrene-butadiene Rubber Containing Silica Nanofiller. *Polymer* **2003**, *44* (20), 6259−6266.
(41) Rizzo, P.; Guerra, G.; Auriemma, F. Thermal Transitions of Polyacrylonitrile Fibers. *Macromolecules* **1996**, *29* (5), 1830−1832.
(42) Devasia, R.; Nair, C. P. R.; Sadhana, R.; Babu, N. S.; Ninan, K. N. Fourier Transform Infrared and Wide-angle X-ray Diffraction Studies of the Thermal Cyclization Reactions of High-molar-mass Poly(acrylonitrile-co-itaconic acid). *J. Appl. Polym. Sci.* **2006**, *100* (4), 3055−3062.
(43) Ouyang, Q.; Cheng, L.; Wang, H.; Li, K. Mechanism and Kinetics of the Stabilization Reactions of Itaconic Acid-modified Polyacrylonitrile. *Polym. Degrad. Stab.* **2008**, *93* (8), 1415−1421.
(44) Fitzer, E.; Müller, D. J. The Influence of Oxygen on the Chemical Reactions During Stabilization of PAN as Carbon Fiber Precursor. *Carbon* **1975**, *13* (1), 63−69.
(45) Rangarajan, P.; Bhanu, V. A.; Godshall, D.; Wilkes, G. L.; McGrath, J. E.; Baird, D. G. Dynamic Oscillatory Shear Properties of Potentially Melt Processable High Acrylonitrile Terpolymers. *Polymer* **2002**, *43* (9), 2699−2709.
(46) Fitzer, E.; Frohs, W.; Heine, M. Optimization of Stabilization and Carbonization Treatment of PAN Fibres and Structural Characterization of the Resulting Carbon Fibres. *Carbon* **1986**, *24* (4), 387−395.
(47) Liu, Y.; Chae, H. G.; Kumar, S. Gel-spun Carbon Nanotubes/Polyacrylonitrile Composite Fibers. Part II: Stabilization Reaction Kinetics and Effect of Gas Environment. *Carbon* **2011**, *49*, 4477−4486.
(48) Schurz, J. Discoloration Effects in Acrylonitrile Polymers. *J. Polym. Sci.* **1958**, *28* (117), 438−439.
(49) Watt, W.; Johnson, W. Mechanism of Oxidisation of Polyacrylonitrile Fibres. *Nature* **1975**, *257* (5523), 210−212.
(50) Nimz, H. A New Type of Rearrangement in the Lignin Field. *Angew. Chem., Int. Ed. Engl.* **1966**, *5* (9), 843−843.
(51) Braun, J. L.; Holtman, K. M.; Kadla, J. F. Lignin-based Carbon Fibers: Oxidative Thermostabilization of Kraft Lignin. *Carbon* **2005**, *43* (2), 385.
(52) Brodin, I.; Ernstsson, M.; Gellerstedt, G.; Sjöholm, E. Oxidative Stabilisation of Kraft Lignin for Carbon Fibre Production. *Holzforschung* **2012**, *66* (2), 141−147.
(53) Foston, M.; Nunnery, G. A.; Meng, X.; Sun, Q.; Baker, F. S.; Ragauskas, A. NMR a critical tool to study the production of carbon fiber from lignin. *Carbon* **2013**, *52* (0), 65−73.
(54) Shimada, I.; Takahagi, T.; Fukuhara, M.; Morita, K.; Ishitani, A. FT-IR Study of the Stabilization Reaction of Polyacrylonitrile in the

DOI: 10.1021/acssuschemeng.5b00562
ACS Sustainable Chem. Eng. 2015, 3, 1943−1954

Production of Carbon Fibers. *J. Polym. Sci., Part A: Polym. Chem.* **1986**, *24* (8), 1989−1995.
(55) Prilutsky, S.; Zussman, E.; Cohen, Y. The Effect of Embedded Carbon Nanotubes on the Morphological Evolution During the Carbonization of Poly(acrylonitrile) Nanofibers. *Nanotechnology* **2008**, *19*, 165603.
(56) Chae, H. G.; Minus, M. L.; Rasheed, A.; Kumar, S. Stabilization and Carbonization of Gel Spun Polyacrylonitrile/Single wall Carbon Nanotube Composite Fibers. *Polymer* **2007**, *48* (13), 3781−3789.
(57) Kubo, S.; Uraki, Y.; Sano, Y. Preparation of Carbon Fibers from Softwood Lignin by Atmospheric Acetic Acid Pulping. *Carbon* **1998**, *36* (7−8), 1119−1124.
(58) Liu, Y.; Chae, H. G.; Kumar, S. Gel-spun Carbon Nanotubes/Polyacrylonitrile Composite Fibers. Part III: Effect of Stabilization Conditions on Carbon Fiber Properties. *Carbon* **2011**, *49*, 4487−4496.
(59) Fischer, L.; Ruland, W. The influence of graphitization on the mechanical properties of carbon fibers. *Colloid Polym. Sci.* **1980**, *258* (8), 917−922.
(60) Ferrari, A. C. Raman Spectroscopy of Graphene and Graphite: Disorder, Electron-phonon Coupling, Doping and Nonadiabatic Effects. *Solid State Commun.* **2007**, *143* (1), 47−57.
(61) Ferrari, A. C.; Robertson, J. Resonant Raman Spectroscopy of Disordered, Amorphous, and Diamondlike Carbon. *Phys. Rev. B: Condens. Matter Mater. Phys.* **2001**, *64* (7), 075414.
(62) Ferrari, A. C.; Robertson, J. Interpretation of Raman Spectra of Disordered and Amorphous Carbon. *Phys. Rev. B: Condens. Matter Mater. Phys.* **2000**, *61* (20), 14095−14107.
(63) Cuesta, A.; Dhamelincourt, P.; Laureyns, J.; Martínez-Alonso, A.; Tascón, J. M. D. Raman Microprobe Studies on Carbon Materials. *Carbon* **1994**, *32* (8), 1523−1532.
(64) Katagiri, G.; Ishida, H.; Ishitani, A. Raman Spectra of Graphite Edge Planes. *Carbon* **1988**, *26* (4), 565−571.
(65) Ishimaru, K.; Hata, T.; Bronsveld, P.; Imamura, Y. Microstructural Study of Carbonized Wood After Cell Wall Sectioning. *J. Mater. Sci.* **2007**, *42* (8), 2662−2668.
(66) Ishimaru, K.; Hata, T.; Bronsveld, P.; Imamura, Y.; Meier, D. Spectroscopic Analysis of Carbonization Behavior of Wood, Cellulose and Lignin. *J. Mater. Sci.* **2007**, *42* (1), 122−129.
(67) Tuinstra, F.; Koenig, J. L. Raman Spectrum of Graphite. *J. Chem. Phys.* **1970**, *53* (3), 1126−1130.
(68) Mallet-Ladeira, P.; Puech, P.; Toulouse, C.; Cazayous, M.; Ratel-Ramond, N.; Weisbecker, P.; Vignoles, G. L.; Monthioux, M. A Raman study to obtain crystallite size of carbon materials: A better alternative to the Tuinstra−Koenig law. *Carbon* **2014**, *80*, 629−639.
(69) Zickler, G. A.; Smarsly, B.; Gierlinger, N.; Peterlik, H.; Paris, O. A Reconsideration of the Relationship Between the Crystallite Size La of Carbons Determined by X-ray Diffraction and Raman Spectroscopy. *Carbon* **2006**, *44* (15), 3239−3246.
(70) Dallmeyer, I.; Lin, L. T.; Li, Y.; Ko, F.; Kadla, J. F. Preparation and Characterization of Interconnected, Kraft Lignin-Based Carbon Fibrous Materials by Electrospinning. *Macromol. Mater. Eng.* **2014**, *299* (5), 540−551.
(71) Ferrari, A. C.; Robertson, J. Raman Spectroscopy of Amorphous, Nanostructured, Diamond−like Carbon, and Nanodiamond. *Philos. Trans. R. Soc., A* **2004**, *362* (1824), 2477−2512.
(72) Rodríguez-Mirasol, J.; Cordero, T.; Rodríguez, J. J. High-temperature Carbons from Kraft Lignin. *Carbon* **1996**, *34* (1), 43−52.
(73) Husman, G. In *Development and Commercialization of a Novel Low-Cost Carbon Fiber*; 2013 DOE Hydrogen and Fuel Cells Program and Vehicle Technologies Program Annual Merit Review and Peer Evaluation Meeting, 2013.
(74) Rahaman, M. S. A.; Ismail, A. F.; Mustafa, A. A review of heat treatment on polyacrylonitrile fiber. *Polym. Degrad. Stab.* **2007**, *92* (8), 1421−1432.
(75) Lyons, K. M.; Newcomb, B. A.; McDonald, K. J.; Chae, H. G.; Kumar, S. Development of Single Filament Testing Procedure for Polyacrylonitrile Precursor and Polyacrylonitrile-based Carbon Fibers. *J. Compos. Mater.* **2015**, *49* (18), 2231−2240.
(76) Chae, H. G.; Newcomb, B. A.; Gulgunje, P. V.; Liu, Y.; Gupta, K. K.; Kamath, M. G.; Lyons, K. M.; Ghoshal, S.; Pramanik, C.; Giannuzzi, L.; Şahin, K.; Chasiotis, I.; Kumar, S. High Strength and High Modulus Carbon Fibers. *Carbon* **2015**, *93*, 81−87.
(77) Kumar, S.; Anderson, D. P.; Crasto, A. S. Carbon Fibre Compressive Strength and Its Dependence on Structure and Morphology. *J. Mater. Sci.* **1993**, *28* (2), 423−439.
(78) Şahin, K.; Fasanella, N. A.; Chasiotis, I.; Lyons, K. M.; Newcomb, B. A.; Kamath, M. G.; Chae, H. G.; Kumar, S. High Strength Micron Size Carbon Fibers From Polyacrylonitrile−Carbon Nanotube Precursors. *Carbon* **2014**, *77*, 442.
(79) Newcomb, B. A.; Chae, H. G.; Gulgunje, P. V.; Gupta, K.; Liu, Y.; Tsentalovich, D. E.; Pasquali, M.; Kumar, S. Stress transfer in polyacrylonitrile/carbon nanotube composite fibers. *Polymer* **2014**, *55* (11), 2734−2743.
(80) Chien, A. T.; Liu, H. C.; Newcomb, B. A.; Xiang, C.; Tour, J. M.; Kumar, S. Polyacrylonitrile Fibers Containing Graphene Oxide Nanoribbons. *ACS Appl. Mater. Interfaces* **2015**, *7* (9), 5281−5288.
(81) Vainio, U.; Serimaa, R.; Maximova, N.; Laine, J.; Stenius, P.; Hortling, B.; Simola, L. K.; Gravitis, J. Morphology of Dry Lignins and Size and Shape of Dissolved Kraft Lignin Particles by X-ray Scattering. *Langmuir* **2004**, *20* (22), 9736−9744.

DOI: 10.1021/acssuschemeng.5b00562
ACS Sustainable Chem. Eng. 2015, 3, 1943−1954